Ecology, 81(10), 2000, pp. 2753–2766

SPATIAL SYNCHRONY OF SPRUCE BUDWORM OUTBREAKS IN EASTERN NORTH AMERICA

DAVID W. WILLIAMS[1] AND ANDREW M. LIEBHOLD[2]

[1]*USDA Forest Service, Northeastern Research Station, 11 Campus Boulevard, Suite 200, Newtown Square, Pennsylvania 19073 USA*
[2]*USDA Forest Service, Northeastern Research Station, 180 Canfield Street Morgantown, West Virginia 26505 USA*

Abstract. We investigated the spatial synchrony of outbreaks of the spruce budworm, *Choristoneura fumiferana,* over much of its outbreak range in eastern North America during the period 1945–1988. Spatial synchrony decreased with distance between local populations and approached zero near 2000 km. Investigation of the synchrony of local population time series with cluster analysis revealed a pattern of geographically distinct blocks of clusters oriented along an east–west axis. Spatial synchrony also was identified in monthly temperature and precipitation time series at 18 weather stations over the same time period and geographical range as the spruce budworm outbreaks. Cross correlations decreased linearly with distance between stations and approached zero near 3000 km and 1800 km, respectively. We developed a spatially explicit lattice model for a single species occupying multiple patches. Within patches, the model had first order logistic dynamics, and patches were linked by dispersal that depended upon their separation distances. Both local and regional stochasticity (i.e., a Moran effect) were present. The modeled lattice had the same spatial configuration as the outbreak region to facilitate investigating the relative effects of a Moran effect and dispersal on spatial synchrony. Simulations with and without a simple region-wide Moran effect and three levels of dispersal did not produce the decrease in spatial synchrony with distance observed with spruce budworm time series. However, when run at the highest dispersal rate, those simulations produced cluster maps similar to that observed for spruce budworm defoliation. Simulations with a spatially autocorrelated disturbance that had either zero or high local variability and three levels of dispersal produced decreases in spatial synchrony with distance similar to that observed in the historical data. When run at the highest dispersal rate, simulations yielded cluster maps similar to the cluster map for defoliation. We discuss the potential significance of the spatially autocorrelated disturbance factor in understanding regional insect outbreaks. We also consider the plausibility of dispersal rates used in our simulations. We suggest in conclusion that spruce budworm outbreaks were synchronized by a combination of a spatially autocorrelated Moran effect and a high dispersal rate.

Key words: Choristoneura fumiferana*; cross correlation; dispersal; forest defoliator outbreaks; lattice model; Moran effect; regional weather patterns; spatial population dynamics; spatial synchrony; spatially autocorrelated disturbance; spruce budworm.*

INTRODUCTION

Recent studies have reported spatial synchrony over a wide range of animal taxa, including moths and butterflies (Thomas 1991, Hanski and Woiwod 1993, Sutcliffe et al. 1996), aphids (Hanski and Woiwod 1993), birds (Ranta et al. 1995*b,* Lindström et al. 1996), and various other vertebrate groups (Ranta et al. 1995*a,* Ranta et al. 1997*b,* Grenfell et al. 1998). Spatial scales for investigating synchrony have ranged from meters to kilometers (Thomas 1991, Sutcliffe et al. 1996) to hundreds of kilometers (Hanski and Woiwod 1993, Ranta et al. 1995*b*) and even to thousands of kilometers (Pollard et al. 1993, Hawkins and Holyoak 1998). Several mechanisms have been proposed to explain spatial synchrony: regional stochasticity (Pollard 1991, Hanski and Woiwod 1993, Ranta et al. 1997*a*), dispersal (Hanski and Woiwod 1993, Ranta et al. 1995*a*), spatially density dependent predation (Ydenberg 1987), and infection by mobile viruses that persist for long periods outside their hosts (Shepherd et al. 1988, Myers 1993). We consider the first two mechanisms to be the most general and pursue them here.

Regional stochasticity is perhaps best exemplified by the ''Moran effect'' (Moran 1953*a, b,* Royama 1992). Moran proposed that local populations of a widespread species that oscillated as a result of stochastic perturbations acting on intrinsic density dependent processes might be synchronized regionally by the influence of a common extrinsic disturbance. In an investigation of the Canadian lynx cycle, Moran (1953*b*) observed that lynx populations oscillated as the result of a process that could ''plausibly be assumed to be due to the intrinsic biological system.'' ''However,'' he continued, ''this does not explain why the oscillations are so clear-

Manuscript received 21 May 1999; revised 20 September 1999; accepted 1 October 1999.

ly and strongly synchronized over the whole of Canada. We therefore inquire whether meteorological phenomena, for which we would expect a considerable degree of correlation over the whole area, could so influence the population densities as to synchronize the cycles.'' The Moran effect has been identified recently to be an important factor in the outbreak synchrony of forest insect populations (Williams and Liebhold 1995, Myers 1998). Dispersal serves to link subpopulations directly through exchange of individuals and leads to spatial synchrony through the smoothing of the variability of local populations (Barbour 1990).

Spatial synchrony has been considered within the context of metapopulation biology recently in part because of its negative implications for conservation ecology. Populations of rare or endangered species that are synchronized regionally are at risk of simultaneous local extinctions that may result in global extinction (Thomas and Hanski 1997). Spatial synchrony is also significant to the management of forest insects, but for the opposite reason. Many species of phytophagous forest insects undergo synchronous population cycles in which outbreaks occur simultaneously over large regions and the spatial extent of damage may have devastating consequences (Myers 1988).

One of the most destructive forest defoliators in North America is the spruce budworm, *Choristoneura fumiferana* (Clemens), a univoltine tortricid moth that feeds on true firs and spruces (Blais 1985, Mattson et al. 1988). The defoliator undergoes population oscillations of 30–35 years, which typically include 5–10 years at high outbreak levels. Numerous hypotheses have been proposed for these population dynamics, including synchrony with the pulsed development of even-aged stands of hosts (Blais 1985); regulation by a suite of specialist parasitoids (Royama 1992) or by an ubiquitous pathogen (Régnière and Lysyk 1995); release from control by periods of weather favorable for population growth and survival, commonly known as the ''theory of climatic release'' (Wellington et al. 1950, Greenbank 1956, Swetnam and Lynch 1993); and the existence of double population equilibria at high and low densities (Clark et al. 1979). Outbreaks typically occur almost simultaneously over wide areas of eastern North America (Hardy et al. 1986). Two hypotheses have been advanced for the regional outbreak patterns: (1) that outbreak populations first develop in areas with susceptible forest stands and disperse subsequently to other areas, which is known as the ''epicenter hypothesis'' (Hardy et al. 1983), and (2) that local populations that oscillate as a result of intrinsic density-dependent factors are synchronized by exposure to a common regional disturbance (Royama 1984, 1992). Thus, current theories of spatial synchrony of spruce budworm outbreaks generally contrast the actions of dispersal and the Moran effect.

In this paper, we investigate spatial synchrony at the landscape scale over thousands of kilometers of the natural outbreak range of spruce budworm. We first examine the empirical evidence for synchrony and then explore its possible causes using simulations of a spatially explicit lattice model that is simple in structure but realistic in its parameterization and spatial configuration. The simulations explore the relative roles of dispersal and the Moran effect. We see such use of a simple yet realistic model of spatially structured populations to explain a phenomenon at the landscape level as a first step in building the bridge between population ecology theory and landscape ecology (Wiens 1997).

Methods

Our approach to understanding spatial synchrony involved a combination of statistics and population modeling. We first analyzed synchrony in spruce budworm defoliation time series using two spatial techniques: cluster analysis and cross correlation analysis. Cluster analysis of the defoliation time series in individual grid cells (Liebhold and Elkinton 1989) enabled us to create maps comparing the similarity of dynamics across eastern North America. Our use of cross correlation analysis involved plotting cross correlations (at time lag zero) of pairs of subpopulations in individual grid cells against the distance between them. Examination of the trend of this relationship has been used to infer the relative roles of dispersal and regional stochasticity in producing spatial synchrony (Hanski and Woiwod 1993). In order to further our understanding of the processes observed in spruce budworm synchrony, we developed a spatially explicit metapopulation model to simulate dynamics at a large spatial scale. We constructed the model with the specific intent of comparing its output with the defoliation data using our two spatial statistical techniques.

Map development

Basic data came from maps of areas defoliated annually by spruce budworm in eastern North America over the period 1945–1988. Maps covered a longitudinal range of 3400 km and a latitudinal range of 1300 km and included the Canadian provinces of Manitoba, Ontario, Quebec, and Newfoundland and the state of Maine (Fig. 1, white areas). Maps from 1945 through 1980 were digitized from paper maps published in Hardy et al. (1986). Maps from 1981 through 1988 were developed by digitizing and compiling defoliation maps obtained from the forestry agencies of individual provinces and states. The annual maps were developed from aerial pest damage surveys and depicted areas with defoliation detectable from the air, which is generally considered to be >30% canopy defoliation (Webb et al. 1961). As a general caveat, the published maps are known to have varied in quality through time as survey techniques improved over the period of the study. In addition, intensity of the surveys varied from area to area and year to year; for example, New Brunswick generally was surveyed more intensively than

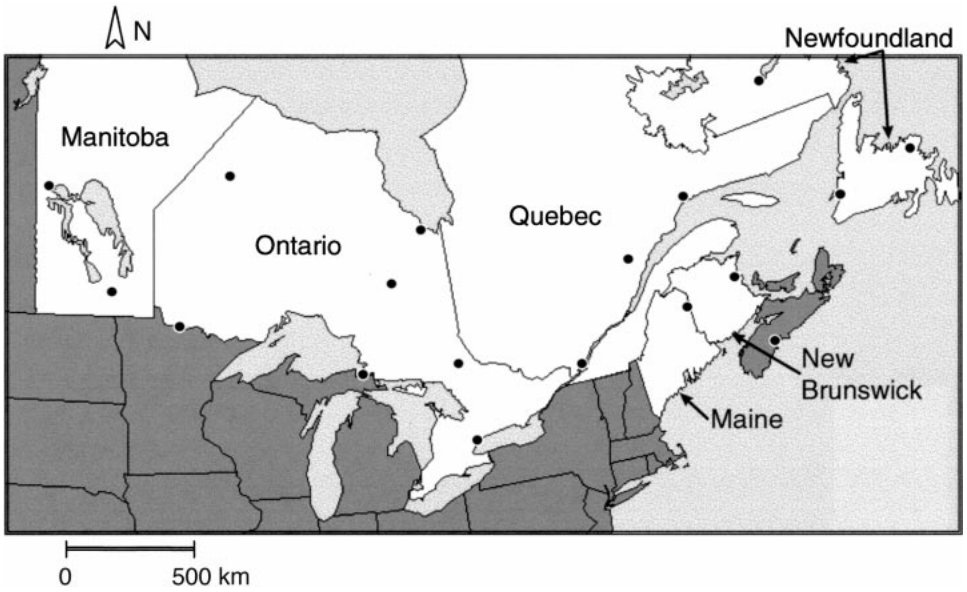

FIG. 1. Area of eastern North America covered in the study (white). Locations of the 18 weather stations with monthly temperature and precipitation means over the period 1945–1988 are indicated by dots.

northern Ontario (Kettela 1983). Details of the digitization and the development of data layers are provided in Williams and Liebhold (1997).

As another caveat, it must be noted that many state and provincial spray programs were carried out against spruce budworm over the time period of the study. In general, a relatively small percentage of the defoliated area was treated with insecticides each year, however. In Quebec, a mean of 10% of the area defoliated annually was treated during the years 1968–1988 (Lachance 1995), whereas in Ontario, a mean of just 0.3% of the area defoliated annually was treated over the years 1974–1987 (Howse 1995, Howse et al. 1995). Moreover, the efficacy of the treatments in preventing defoliation is not known. Thus, it is unlikely that the spray programs had much impact on the defoliation data used here.

Digitized maps were 761 column by 373 row grids of small unit cells, which represented ground surface areas $\sim 5 \times 5$ km in extent. Individual cells were assigned a value of 1 if the corresponding forest area was defoliated and 0 if not defoliated. For analyzing synchrony, unit cells were aggregated to produce larger square cells consisting of 32×32 unit cells (i.e., 160×160 km). Defoliation values of the larger cells were simply the sums of the component unit cells, up to a maximum of 1024. When the aggregated annual maps were superimposed in temporal sequence, serial sequences of annual values produced time series of defoliation for individual cells. Time series that contained <4 yr of defoliation values >0 (i.e., $<9\%$ of the 44 years) were excluded from analyses. Following the general practice for population time series, defoliation values were transformed as $\ln(n + 1)$ before analysis (Royama 1992).

Weather patterns were analyzed to characterize the strength of regionally correlated factors extrinsic to spruce budworm populations. Weather records were obtained for 18 stations that covered the study region and included monthly average temperature and precipitation for each year over the time period 1945–1988 (Fig. 1). Data came ultimately from the U.S. National Climatic Data Center in Asheville, North Carolina, and were provided by Spangler and Jenne (1990).

Statistical analyses

Variables used for the cluster analysis were the 44 years of defoliation values among the 85 grid cells. Before analysis, variables were standardized to a mean of 0.0 and a standard deviation of 1.0 to avoid the undue influence of years with high defoliation on the cluster algorithm (SAS Institute 1990). Ward's minimum variance method was used to identify clusters (Ward 1963). At each step of the analysis, all possible pairs of clusters were compared with respect to their error sums of squares and the pair that minimized the increase in that quantity was joined as a single cluster (Everitt 1980). The minimum number of clusters determined was four. A higher resolution map with cells consisting of 8×8 aggregates of the basic unit cells (i.e., 40×40 km in size) also was analyzed to investigate possible effects of spatial resolution on patterns of spatial synchrony.

Evaluating the various model scenarios (q.v., *Methods: Spatial population model*) as explanations of the observed synchrony of spruce budworm defoliation ne-

cessitated comparing cluster maps. Rather than relying on subjective impressions of the similarity of cluster patterns, we used cell by cell correlations of the cluster values as a measure of similarity between maps. We were not interested in absolute values of the clusters, but only in their qualitative geographical patterns. Thus, we considered all 24 permutations of the four cluster numbers for the defoliation map. For each model comparison, we computed the 24 Pearson correlations between the defoliation map permutations and the map of the model scenario. We then selected the highest correlation as the similarity index for that comparison.

The second technique for analyzing spatial synchrony involved the use of a ''prewhitening'' procedure for the removal of serial correlation prior to the cross correlation analysis (Box and Jenkins 1976). First, the time series were diagnosed for the presence of autoregressive structure and, if present, for its order by examining the partial autocorrelation function (Box and Jenkins 1976). An appropriate model was then estimated for each series. Eleven time series were diagnosed with significant first and second order partial autocorrelations and fitted with the second order autoregressive model, $X(t) = a_0 + a_1X(t - 1) + a_2X(t - 2)$. The remaining 74 series were fitted with the first order autoregressive model, $X(t) = a_0 + a_1X(t - 1)$. Residual series were computed for each defoliation series by subtracting the observed values from those predicted by the autoregressive model. Next, cross correlations (i.e., Pearson correlations at lag 0) were computed for all the pairs of residuals series. Finally, the cross correlations of all pairs were plotted against the distances between cells, and linear regressions of the cross correlations on distance were computed. We acknowledge that such regression analyses are not strictly valid statistically because cross correlations are not independent observations. Nevertheless, the analyses likely provided reasonable estimates of slope and intercept values of the relationship, which we used primarily to compare the results of several model simulations and the observations. We were less interested in testing the significance of the regressions, which is known to be affected by the lack of independence (Dennis and Taper 1994).

The techniques of plotting cross correlations against distance and computing linear regressions were also applied to the monthly weather time series. The temperature and precipitation time series were used directly for computing cross correlations, as they had no detectable autoregressive structure and were diagnosed as essentially random series. We did not attempt to estimate the relationship between weather and spruce budworm outbreaks directly. That relationship may be very complex and therefore unlikely to be characterized only from historical outbreak data.

Spatial population model

Our model is from a general class known as ''spatially explicit metapopulation models.'' Following the terminology of Hanski and Simberloff (1997), a metapopulation is ''a set of local populations within some larger area, where typically migration from one local population to at least some other patches is possible.'' Within the metapopulation context, a spatially explicit model is one ''in which migration is distance-dependent, often restricted to the nearest habitat patches . . . ''. Hanski and Simberloff (1997) also refer to a model such as ours, in which the patches are typically identical cells on a regular grid and population size in a patch is a continuous variable, as a ''lattice model,'' the term that we will use in the remainder of the paper.

We chose a first-order logistic model to describe population dynamics in individual cells:

$$N_i(t) = \alpha_0 + N_i(t - 1) - \exp[\alpha_1 - \alpha_2 N_i(t - 1)] + \sum_{j=1}^{m} N_{ji}(t) + w_i(t),$$

where $N_i(t)$ is the logarithm of population numbers in cell i at time t, $N_{ji}(t)$ is the log of numbers dispersing from cell j to cell i at time t, and $w_i(t)$ is the stochastic disturbance in cell i at time t. This model, minus the immigration term, was modified from Royama (1992: Eq. 5.15). Our modification was to drop the $N_i(t - 2)$ term because previous analysis of spruce budworm dynamics (D. Williams and A. Liebhold, *unpublished manuscript*) had not revealed significant second-order effects. We fit the model to the time series of spruce budworm defoliation summed over all of North America and scaled to the individual grid cell level by dividing by 85 (i.e., the number of cells with defoliation). We used the multivariate secant method (Ralston and Jennrich 1978) as implemented in SAS (SAS Institute 1990) to fit the parameters. The resulting parameters used in all simulations were as follows: $\alpha_0 = 1.728$, $\alpha_1 = 0.363$, and $\alpha_2 = -0.046$. At each iteration of the simulation, the populations, $N_i(t)$, in all cells were calculated from their previous values, $N_i(t - 1)$, before any dispersal took place.

The population in each cell was initialized as

$$N_i(0) = 2 + z_i$$

where z_i is an independent uniform random variable over the range 0 to 1. The model was run for 4000 iterations, and the final 200 iterations were used for analyses.

The dispersal model had populations from each cell dispersing to all the other m cells in each time interval with rates decreasing exponentially with the distance between cells (Hanski and Woiwod 1993):

$$N_{ji}(t) = N_j(t)\cdot\kappa\cdot\exp[-\delta x_{ji}] \Big/ \sum_{j=1}^{m} \exp[-\delta x_{ji}],$$

where x_{ji} is the distance between cells j and i, κ is the proportion of population N_j emigrating at time t, and δ is the dispersal rate parameter. Because the relative

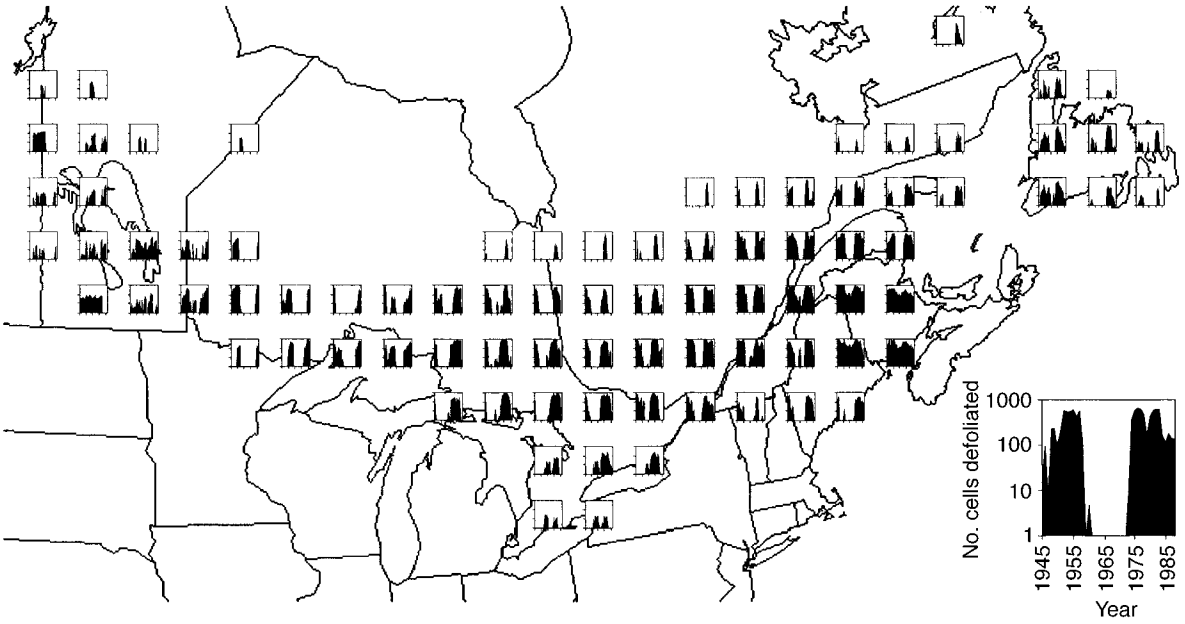

FIG. 2. Time series of detectable defoliation by eastern spruce budworm in 160 × 160 km cells in eastern North America over the 44-yr period from 1945 to 1988. The large cell at the lower right provides a key.

dispersal rate was modeled as a negative exponential function, a small value of δ resulted in a long dispersal distance. Following Hanski and Woiwod (1993), we simulated a high dispersal rate scenario with $\kappa = 0.5$ and $\delta = 0.2$ and a low dispersal rate scenario with $\kappa = 0.1$ and $\delta = 2.0$.

To facilitate qualitative comparisons between real world and model results, the spatially explicit lattice model was laid out like that of the spruce budworm defoliation map (Fig. 2), with 85 cells containing populations distributed over a grid of 23 columns and 11 rows in the same spatial orientation. A line map of eastern North America was laid over the results of cluster analyses of model output to permit comparisons with the defoliation map. In addition, we rescaled the results of other analyses of model scenarios to real world dimensions using 160 km as our basic cell size.

Disturbance models

The stochastic disturbance variable was formulated in several ways to investigate the effects of a purely local disturbance, a region-wide disturbance, and a disturbance with varying degrees of spatial autocorrelation within the region. Purely local and region-wide disturbances were formulated as follows:

$$w_i(t) = \beta_0 (\beta_1 f_i(t) + (1 - \beta_1) g(t))$$

where $f_i(t)$ is the disturbance in cell i at time t and $g(t)$ is the regional disturbance common to all $m + 1$ cells. Values of $f_i(t)$ and $g(t)$ were drawn from a normal distribution with a mean of 0.0 and variance of 1.0. The scaling parameter, β_0, was fixed at 0.1, while the parameter, β_1, was set at 1.0 to simulate a purely local disturbance. We set β_1 at 0.5 to simulate the Moran effect, assuming that it would be composed reasonably of half local disturbance and half regional disturbance.

We developed a spatially autocorrelated disturbance term using unconditional sequential Gaussian simulation, a geostatistical technique for simulating maps with specific spatial structure (Deutsch and Journel 1992, Goovaerts 1997). In all we simulated 4000 grids of 23 × 11 values of a normally distributed random variable (mean = 0.0, variance = 1.0) with specific autocorrelation structure. Sequential Gaussian simulation uses simple kriging as the basis for determining values assigned to individual grid cells. Simple kriging is a technique from geostatistics that estimates the value of a variable at a specific location as a weighted linear combination of values at nearby locations while minimizing error variance (Isaaks and Srivastava 1989). Simulation of a single grid started with random selection of a cell, which was assigned a value at random from a normal distribution. A second cell was located at random and a mean and variance were assigned by kriging from the estimate at the first cell. The mean and variance were used to form a conditional cumulative distribution function, and the value of the cell was drawn at random from that distribution. Subsequent cells were located on a random path through the grid and assigned values by kriging and conditioning with estimates and variances obtained for all previous cells, and the process ended when all cells were assigned values (Goovaerts 1997).

The basis for weighting in simple kriging is the variogram, $\gamma(h)$, which for sample data represents the variance between M pairs of points h distance units apart:

$$\gamma(h) = \frac{1}{2M(h)} \sum_{(i,j)|h_{ji}=h} (v_j - v_i)^2$$

(Isaaks and Srivastava 1989). Because we had no data and were interested only in grids of values of a spatially autocorrelated random variable to serve as model input, we used an exponential function as the model for our variogram:

$$\gamma(h) = C(1 - \exp[-h/A])$$

where the parameter A defines the distance (''range'' in geostatistical terms) over which γ approaches its asymptotic value (''sill''), C, which is the maximum variance over the grid of cells (Isaaks and Srivastava 1989, Deutsch and Journel 1992). Ninety-five percent of the maximum variance is reached at a distance of $3A$. Variance at zero distance is obviously zero in this formulation. Because we wanted to investigate the effects of local variation in the disturbance term, we incorporated a ''nugget effect,'' C_0, to produce nonzero variance at short distances, which resulted in the final variogram model:

$$\gamma(h) = \begin{cases} 0 & \text{if } h = 0 \\ C_0 + C_1(1 - \exp[-h/A]) & \text{if } h > 0 \end{cases}$$

(Isaaks and Srivastava 1989). For use in the lattice model, we simulated two cases of spatially autocorrelated random variables (i.e., 8000 simulations in all) produced by combinations of two values of C_0. C_0 equal to 0.5 yielded a strong local disturbance effect, whereas C_0 equal to 0.0 yielded no local disturbance. We set A equal to 5 grid cell widths. Thus, the range of the regional spatially autocorrelated disturbance effect was ~800 km in real world terms.

Results

Spatial synchrony

Time series of spruce budworm defoliation across eastern North America generally exhibited two peaks, from ~1945 to 1955 and from ~1970 to 1985, with a trough during most of the 1960s (Fig. 2). However, the basic pattern was variable, with broad peaks nearly coalescing into a continuous outbreak in Maine and New Brunswick and narrow peaks having wide separation in northern and western parts of Ontario and Quebec. Variability was also apparent in the timing of peaks; the beginnings and ends of outbreaks shifted over the geographical range. The basic pattern often broke down toward the margins of the outbreak range, with single peaks only in some northern areas and choppy series of multiple small peaks in Manitoba and Newfoundland.

The cluster analysis detected a distinct geographical pattern among the time series (Fig. 3a). Three clusters lay in discrete blocks along an east–west axis. The remaining cluster (i.e., cluster 1) consisted of groups of cells scattered around the margins of the outbreak range. Cluster 1 apparently included the less distinctly bimodal time series noted at the margins in Fig. 2. The basic pattern was confirmed at the higher resolution of 40 × 40 km (Fig. 3b). Although the actual cluster numbers were rearranged, the east–west orientation of clusters 2, 3, and 4 was obvious, and cells belonging to cluster 1 were scattered at the margins of the distribution. Thus, spatial scale did not appear to affect the basic patterns of the time series or the clustering procedure.

Overall spatial synchrony was apparent in the cross correlation plot (Fig. 4a). Because the considerable number of points ($n = 3570$) made it difficult to ascertain the exact nature of the relationship, we summarized the cross correlations by computing their means and 95% confidence intervals at 200 km intervals (Fig. 4b). Cross correlations were highest at short distances and decreased steadily at longer ones. A linear regression analysis confirmed the basic pattern, yielding the equation $y = -0.00008x + 0.175$. Using the slope and intercept, the x intercept of the regression equation was calculated as 2080 km, which provided a crude estimate of the range of spatial synchrony.

Spatial synchrony was clearly defined in the cross correlation plots for the monthly weather time series. As ''best'' examples, we have used the November time series (Fig. 5), which had the highest correlations overall. The graphs for the other months were very similar qualitatively to those for November in all cases, however. Cross correlations for the November temperature time series were near 1 at the closest stations and decreased in an approximately linear fashion with distance (Fig. 5a). Cross correlations for the November precipitation time series exhibited a similar pattern, but had lower values overall and a more shallow slope (Fig. 5b). Regression analyses for all months bore out the generally linear patterns (Table 1). The calculated x intercepts for the temperature equations averaged 3094 km ($s = 465.5$) and ranged from 2456 to 4091 km, whereas the precipitation x intercepts averaged 1851 km ($s = 168.6$) and ranged from 1517 to 2150 km. Thus, the range of spatial synchrony appeared to be wider for the temperature time series than for the defoliation time series, and narrower for the precipitation time series. Overall the results are consistent with the general observation that precipitation is more variable spatially than temperature (Mearns et al. 1984).

Lattice model simulations

Cluster analyses of the simulated time series exhibited a wide range of patterns when the spatially explicit lattice model was run under combinations of three levels of dispersal and two types of stochastic disturbance (Fig. 6). Without dispersal, cells were distributed in an apparently random pattern for both disturbance types (Fig. 6a and b). The maximum Pearson correlations were lowest for these cases, suggesting that the cluster patterns were rather unlike the pattern of the defoliation

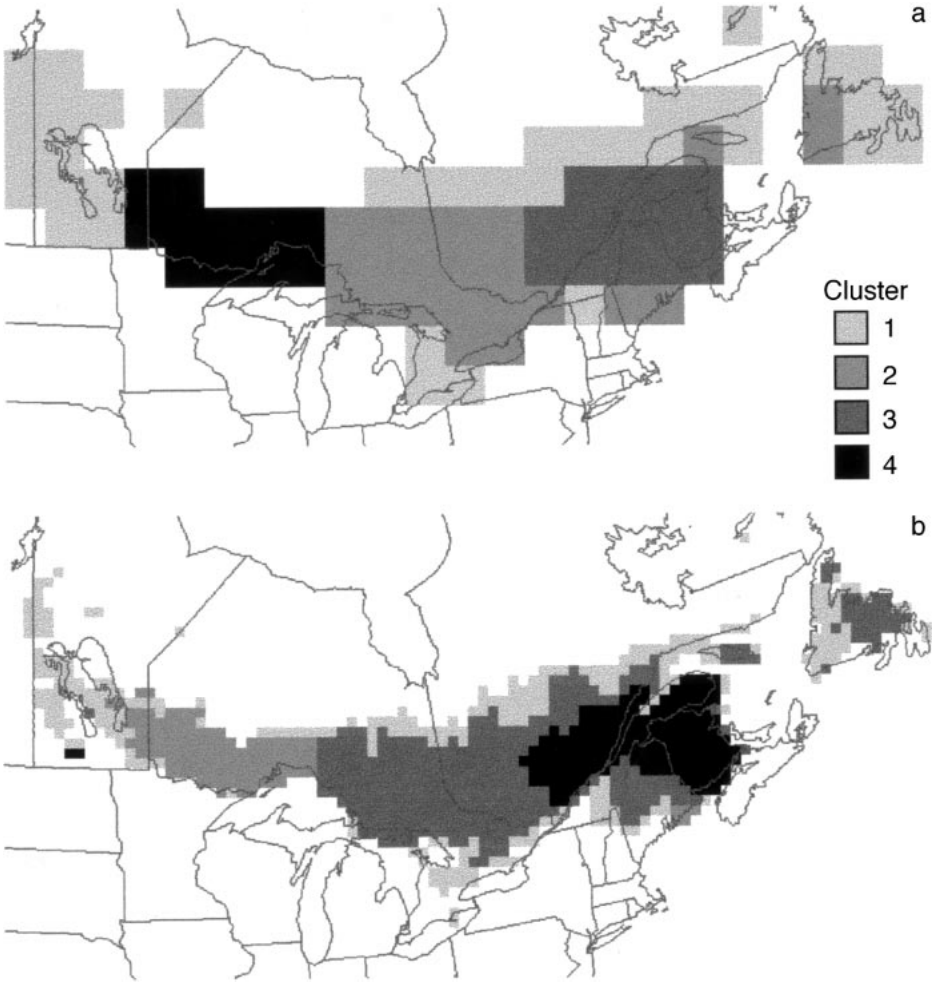

FIG. 3. Clusters of ln-transformed defoliation time series: (a) 160 × 160 km, (b) 40 × 40 km.

series (Table 2). With a low dispersal rate, maps for both disturbance types were dominated by cluster A (Fig. 6c and d), which contained the majority of cells, and had cells of the other clusters scattered primarily around the margins of the distribution. At the high dispersal rate, a distinct pattern emerged: cells were more uniformly distributed among clusters, and, within an area the size and shape of the study area, clusters were arranged along a horizontal (i.e., ''east–west'') axis (Fig. 6e and f). The pattern resembled a ''target'', with concentric rings of clusters surrounding a central ''bull's-eye''. As such the pattern was similar spatially to the cluster map for the defoliation time series (cf. Fig. 3a). This impression was confirmed by the maximum Pearson correlations (Table 2), which were highest between the cluster patterns for defoliation data and those simulations at the high dispersal rate.

Cross correlation patterns varied considerably depending upon the combination of dispersal parameters and disturbance types, whether a purely local effect or a global Moran effect (Fig. 7). (Note that we will refer to a Moran effect that acts uniformly over the study region as a ''global'' effect, to distinguish it from the spatially autocorrelated Moran effect that acts at a smaller spatial scale.) Model simulations with the global Moran effect (Fig. 7, closed symbols) had higher cross correlations, as indicated by their intercepts, and generally lower variability than those with a local disturbance (Fig. 7, open symbols; Table 3). Increasing the dispersal rate from low to high resulted in a strong increase in the r^2 value for the relationship between spatial synchrony and distance for each disturbance type. The combinations with the high dispersal rate exhibited decreases in slopes of cross correlation with distance (Table 3) as compared with the low dispersal rate. However, those negative slopes were relatively small in magnitude (Fig. 7c) and not nearly as strong as that observed for the defoliation data (cf. Fig. 4b).

The observation that cross correlations of temperature and precipitation variables among weather stations decreased with distance and reached zero well within the bounds of the study region (Table 1) suggested that

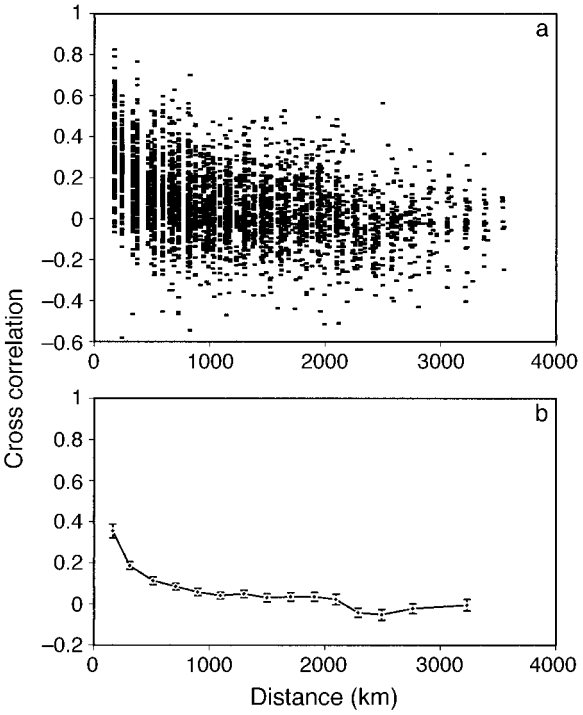

FIG. 4. Relationship between the cross correlations of defoliation residuals and distance: (a) original data, (b) means and 95% confidence intervals of cross correlations at 200-km intervals.

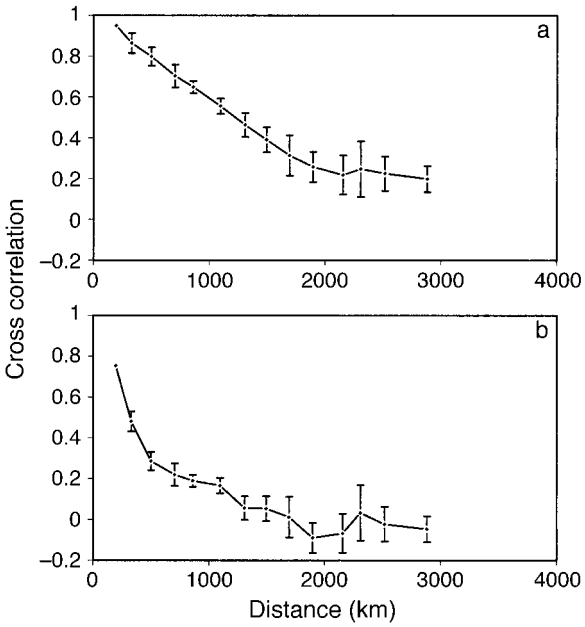

FIG. 5. Relationship between the cross correlations of the annual time series of mean monthly weather variables and distance over the period 1945 through 1988 in eastern North America. Error bars are the 95% confidence intervals for mean cross correlations calculated at 200-km intervals. (a) November temperature, (b) November precipitation.

a Moran effect might be autocorrelated at a spatial scale somewhat smaller than the entire region. To explore this possibility, we ran a second set of lattice model simulations with the two sets of spatially autocorrelated random variables as disturbance terms and the three dispersal rates used previously. Cluster analysis of the simulations without a ''nugget'' effect (i.e., with low local variability) and without dispersal exhibited distinct regional blocks without overlap (Fig. 8b). Simulations with a nugget effect and without dispersal clustered less distinctly and displayed more local stochasticity (Fig. 8a). With the addition of dispersal, the cluster patterns became similar to those observed in the first set of simulations (cf. Fig. 8c–f and Fig. 6c–f). Note again that the target-like cluster patterns under the high dispersal rate (Fig. 8e–f) were remarkably similar to that of the defoliation data (Fig. 3a) and that this similarity was confirmed by the maximum Pearson correlations (Table 4), which were highest for these scenarios.

By contrast with the first set of simulations, the second set generally exhibited a strong inverse relationship between cross correlation and distance (Fig. 9),

TABLE 1. Regression analyses of the cross correlations of mean monthly temperatures and precipitation in eastern North America during the period 1945–1988 on distance (km) between stations (n = 153).

	Temperature				Precipitation			
Month	Slope	Intercept	r^2	x intercept	Slope	Intercept	r^2	x intercept
January	−0.00035	0.911	0.736	2603	−0.00017	0.316	0.260	1836
February	−0.00023	0.929	0.612	4039	−0.00015	0.322	0.216	2150
March	−0.00029	0.993	0.763	3424	−0.00019	0.356	0.377	1866
April	−0.00028	0.879	0.741	3139	−0.00015	0.273	0.256	1857
May	−0.00032	0.888	0.581	2775	−0.00022	0.369	0.428	1661
June	−0.00033	0.806	0.683	2442	−0.00014	0.256	0.240	1871
July	−0.00030	0.850	0.721	2833	−0.00008	0.115	0.096	1517
August	−0.00028	0.882	0.517	3150	−0.00012	0.209	0.207	1714
September	−0.00035	0.982	0.850	2806	−0.00013	0.241	0.258	1884
October	−0.00031	0.995	0.738	3210	−0.00021	0.385	0.410	1850
November	−0.00030	0.903	0.801	3010	−0.00020	0.391	0.435	1937
December	−0.00026	0.950	0.748	3654	−0.00014	0.292	0.225	2070

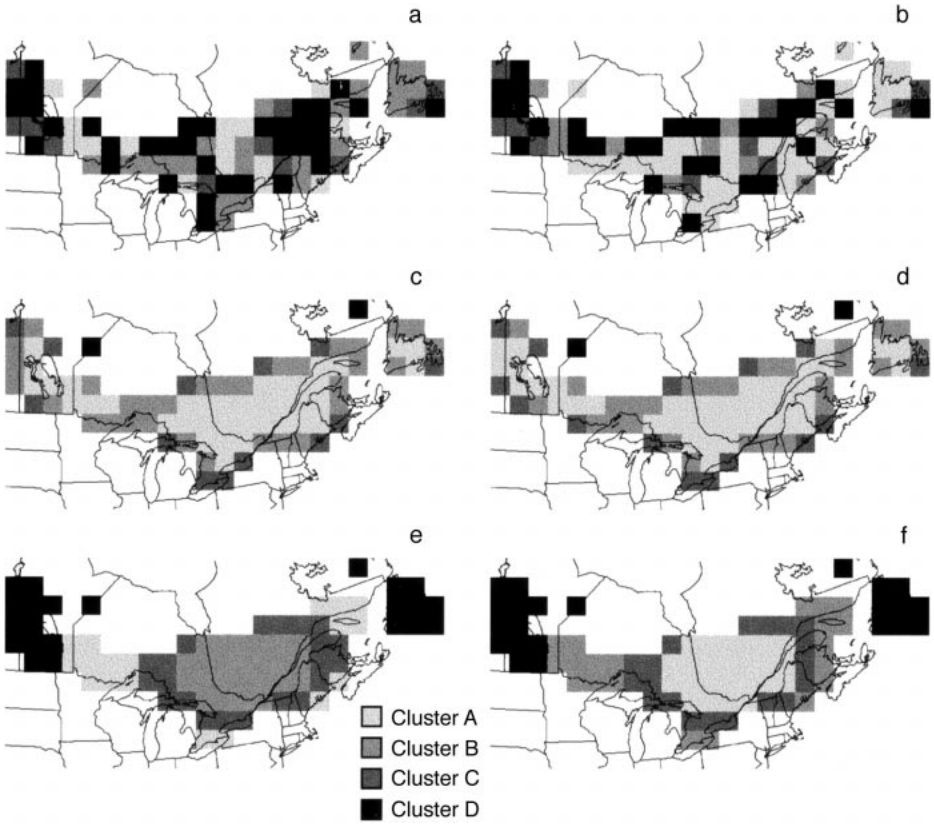

FIG. 6. Clusters of time series simulated with a first-order logistic population model under several combinations of dispersal rates and stochastic disturbances: (a) no dispersal and local disturbance, (b) no dispersal and global Moran effect, (c) low dispersal rate and local disturbance, (d) low dispersal rate and global Moran effect, (e) high dispersal rate and local disturbance, (f) high dispersal rate and global Moran effect.

and regression analyses of those variables had generally high r^2 values (Table 5). Simulations with a nugget effect of 0.5 (i.e., with high local variability) had lower cross correlations than did those without a nugget effect, as evidenced by their regression intercepts. In addition, distance explained much less of the variation in cross correlations in simulations with a nugget effect than in those without, as seen by comparing sets of r^2 values (Table 5). For both disturbance types (Fig. 9), cross correlations increased as the dispersal rate increased. However, the differences between intercepts for the zero and low rate were relatively small in these cases. The r^2 values of the regression of cross correlation on distance increased likewise with increases in the dispersal rate. Of all the cases shown, those with a nugget effect of 0.5 (Fig. 9, open symbols) were most similar visually to the plot of the defoliation data (cf. Fig. 4b). In addition, the cases without a nugget effect (Fig. 9, closed symbols) were curiously similar in appearance to the cross correlation plots of November temperature and precipitation data (Fig. 5) because their y intercepts were high and cross correlations decreased rapidly toward zero with increasing distance.

TABLE 2. Maximum Pearson correlations between cluster values for spruce budworm defoliation (Fig. 3a) and lattice model simulations at six combinations of dispersal rate and disturbance type (Fig. 6) ($n = 85$).

Dispersal rate	Disturbance type	r
0	local	0.277
0	global	0.333
low	local	0.429
low	global	0.385
high	local	0.515
high	global	0.533

DISCUSSION

The spatial synchrony exhibited by spruce budworm was comparable to that reported for other species of Lepidoptera. Although the y intercept of the regression of cross correlation on distance was rather low (0.175), the average of cross correlations at distances up to 200 km was 0.355 (Fig. 4b), which was well within the ranges reported for moth ($\approx$0.3 by Hanski and Woiwod [1993]) and butterfly (0.11–0.44 by Sutcliffe et al. [1996]) populations over the same geographical range. Cross correlations in defoliation by spruce budworm decreased with distance, dropping nearly to zero by

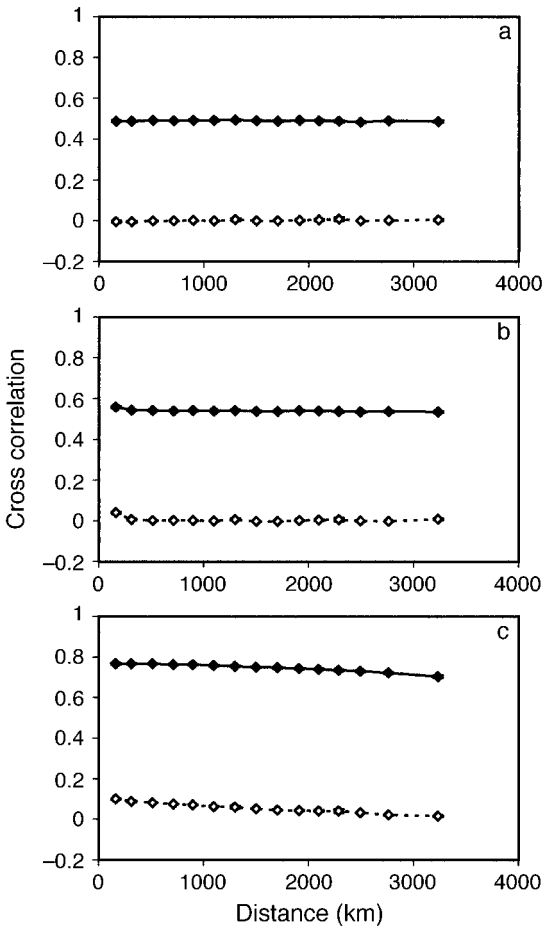

FIG. 7. Relationship between the cross correlations of residuals of population time series and distance for series simulated with a first-order logistic population model under several combinations of dispersal rates and stochastic disturbances. Means and 95% confidence intervals of cross correlations at 200-km intervals are plotted, although the confidence intervals are too narrow to be observed. (a) No dispersal with a local disturbance (open symbol) and a global Moran effect (solid symbol), (b) low dispersal rate with a local disturbance (open symbol), and a global Moran effect (solid symbol), (c) high dispersal rate with a local disturbance (open symbol) and a global Moran effect (solid symbol).

~2000 km. Studies of other taxa have typically reported a much more rapid decrease with distance, with cross correlations of close to zero at <800 km for moths (Hanski and Woiwod 1993) and <300 km for butterflies (Sutcliffe et al. 1996). In the extreme, individual butterfly species exhibited spatial synchrony at ranges of only a few kilometers (Sutcliffe et al. 1996). This has been attributed to the generally sedentary nature of many butterfly species. By contrast, spruce budworm is a very mobile species and disperses readily (Greenbank et al. 1980).

The results of our first set of lattice model simulations confirmed our expectations based on conceptual models. A global Moran effect generally increased spatial synchrony and reduced its variability as compared with a purely local disturbance. An increasing dispersal rate also increased spatial synchrony. However, the relationship between spatial synchrony and distance between populations did not conform with theoretical expectations or with our observations for spruce budworm (Fig. 4). Ranta et al. (1995*a*) outlined two alternative expectations for that relationship. If dispersal serves to link local populations and thereby increase their synchrony, spatial synchrony should decline as the distance between populations increases. If, on the other hand, global stochasticity drives synchrony, spatial synchrony should not decline with distance between local populations. Those expectations are certainly reasonable and were borne out by simulations reported by Hanski and Woiwod (1993) and Ranta et al. (1995*a*). However, despite some significant negative slopes when dispersal was included (Table 3), our simulations did not indicate any strong decrease in spatial synchrony with distance (Fig. 7). One possible explanation was that the levels of variation in the local and global disturbances in our model obscured the more subtle effects of dispersal, a possibility that has been explored theoretically by Haydon and Steen (1997). Another possible explanation was the parameter values used for the population model. We used fitted values, which may not have produced the complex population dynamics necessary to yield such a strong negative effect. Indeed, Hanski and Woiwod (1993) reported a strong decrease of spatial synchrony with distance only in simulations with high dispersal rate and an intrinsic rate of increase in the range that generated chaos. In a similar vein, spatial synchrony is also known to increase in prevalence as the amplitude of population oscillations increases (Barbour 1990).

Alternatively, it is possible that factors other than dispersal may have produced the inverse relationship apparent in Fig. 4. Monthly temperature and precipitation time series exhibited spatial synchrony across eastern North America (Fig. 5, Table 1). Cross correlations decreased strongly with distance and reached zero over a range of 1500–4000 km. Because weather variables have often been implicated as the regional stochasticity driving the Moran effect (Moran 1953*b*, Williams and Liebhold 1995, Hawkins and Holyoak 1998, Myers 1998), our results suggested that such

TABLE 3. Linear regression analyses of cross correlations between pairs of simulated populations and the distances separating them (n = 3570).

Dispersal rate	Disturbance type	Slope	Intercept	r^2
0	local	0.000002	−0.002	0.001
0	global	−0.000001	0.492	<0.001
low	local	−0.000004	0.008	0.002
low	global	−0.000003	0.544	0.003
high	local	−0.000027	0.096	0.081
high	global	−0.000019	0.777	0.182

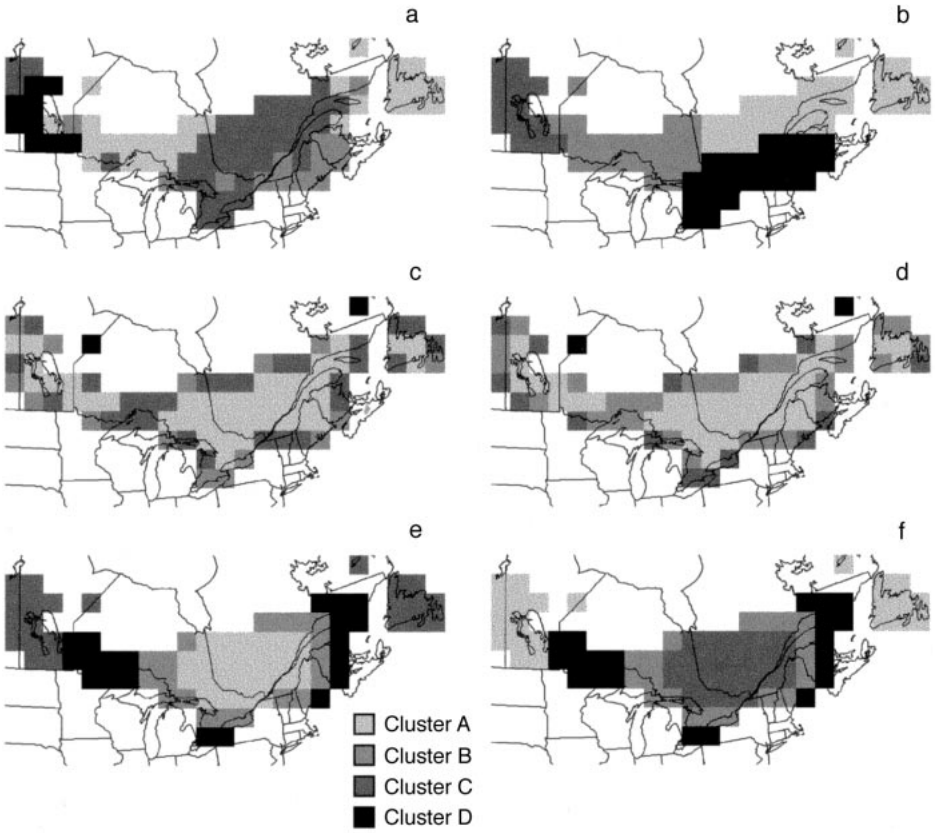

FIG. 8. Clusters of time series simulated with a first-order logistic population model under several combinations of dispersal rates and spatially autocorrelated stochastic disturbances: (a) no dispersal and a nugget effect of 0.5, (b) no dispersal and no nugget effect, (c) low dispersal rate and a nugget effect of 0.5, (d) low dispersal rate and no nugget effect, (e) high dispersal rate and a nugget effect of 0.5, (f) high dispersal rate and no nugget effect.

regional stochasticity may also be autocorrelated spatially. The large-scale synoptic weather patterns to produce such effects have been demonstrated in the meteorological literature (Walsh et al. 1982). Given this evidence, we incorporated a spatially autocorrelated Moran effect into our second set of simulations. Those simulations produced results broadly similar to results of the first set. That is, spatial synchrony generally increased with a strong Moran effect (i.e., as simulated with a zero nugget effect) and a higher dispersal rate, whereas the variability of spatial synchrony decreased with a strong Moran effect. However, the second set of simulations differed in exhibiting a strong decrease of spatial synchrony with distance in all cases.

TABLE 4. Maximum Pearson correlations between cluster values for spruce budworm defoliation (Fig. 3a) and lattice model simulations at six combinations of dispersal rate and disturbance type (Fig. 8) ($n = 85$).

Dispersal rate	Nugget effect	r
0	0.5	0.237
0	0	0.288
low	0.5	0.386
low	0	0.418
high	0.5	0.548
high	0	0.545

The similarity of spatial synchrony patterns between our second set of simulations and spruce budworm defoliation suggests that spatial autocorrelation of environmental stochasticity may cause the pattern of decrease of cross correlations with distance. Thus, we propose that the spatial scale of weather deviation should be an important consideration in future studies of the effects of weather on spatial synchrony of insect outbreaks via the Moran effect. The spatial scale of weather anomalies can be explained by large-scale air movements and other meteorological phenomena (Walsh et al. 1982). The results presented here indicate that the scale of meteorological processes may be important in determining the spatial extent of synchronous insect outbreaks. Although it may be impossible in many cases to identify precisely what weather characteristics are responsible for synchrony, it may be possible to characterize the spatial scale of weather anomalies and relate them to spatial synchrony of insect populations.

Whereas the effect of increasing dispersal rate was

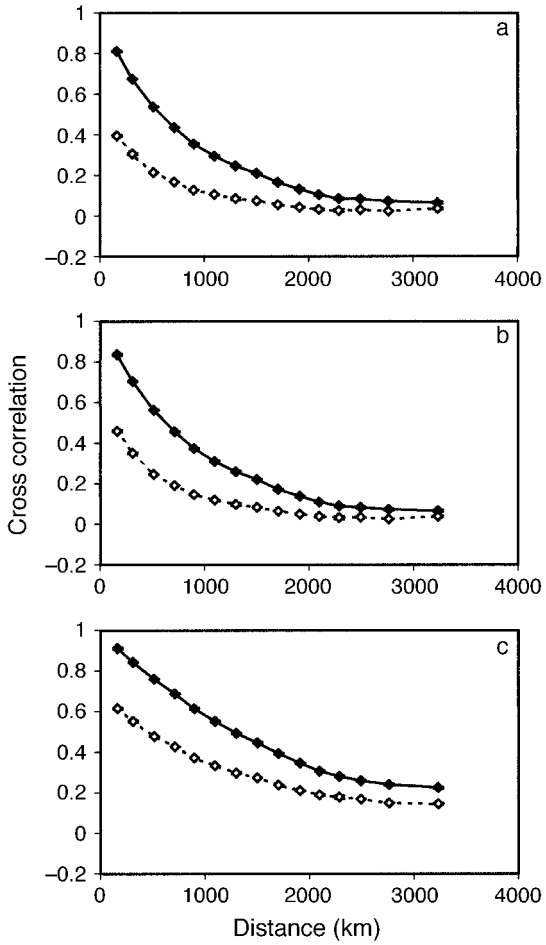

FIG. 9. Relationship between the cross correlations of residuals of population time series and distance for series simulated with a first-order logistic population model under several combinations of dispersal rates and spatially autocorrelated stochastic disturbances. Means and 95% confidence intervals of cross correlations at 200-km intervals are plotted, although the confidence intervals are too narrow to be observed. (a) No dispersal with a nugget effect of 0.5 (open symbol) and no nugget effect (solid symbol), (b) low dispersal rate with a nugget effect of 0.5 (open symbol) and no nugget effect (solid symbol), (c) high dispersal rate with a nugget effect of 0.5 (open symbol) and no nugget effect (solid symbol).

generally to increase the magnitudes of the cross correlations, varying dispersal rate did not change the basic inverse relationship of spatial synchrony to distance. However, dispersal rate did have a distinct effect in changing the qualitative patterns of outbreak synchrony as revealed through cluster analyses. At the high dispersal rate, cluster maps converged in all cases to the east–west target pattern of clusters (Figs. 6e and f, 8e and f) that we have noted as qualitatively similar to the cluster pattern of the defoliation time series (Fig. 3a). Thus, it may be useful to compare the low and high dispersal rates in more detail. Calculating with the exponential dispersal function (see *Methods*) and multiplying by the cell width of 160 km, the distance corresponding to 0.5 relative dispersal (i.e., the median) was 55.5 km at the low rate ($\delta = 2.0$) and 555 km at the high rate ($\delta = 0.2$). Although these estimates are admittedly rough, one may ask if they are at least plausible.

TABLE 5. Linear regression analyses of cross correlations between pairs of simulated populations and the distances separating them ($n = 3570$).

Dispersal rate	Nugget effect	Slope	Intercept	r^2
0	0.5	−0.000111	0.272	0.502
0	0	−0.000250	0.645	0.798
low	0.5	−0.000128	0.311	0.540
low	0	−0.000261	0.674	0.810
high	0.5	−0.000166	0.552	0.756
high	0	−0.000254	0.868	0.912

Spruce budworm is known to be a strong disperser, particularly from forest stands that have at least light levels of defoliation (Greenbank et al. 1980). After remaining in the host stands in which they emerged for about two days and expending about half of their egg complements, females frequently emigrate in mass flights in which they are carried by wind currents. Mean movement rates are ~40 km/hr and typical night flights may carry moths hundreds of kilometers (Greenbank et al. 1980). Flight has been documented from New Brunswick to Newfoundland, a distance of ~450 km (Dobesburger et al. 1983). Thus, dispersal rates used in the spatially explicit model provide plausible ranges of dispersal by spruce budworm moths, and actual dispersal rates probably lie between our high and low parameter values (i.e., 555 km and 55.5 km over a generation, respectively).

In conclusion, spruce budworm outbreaks clearly were synchronized spatially across eastern North America. By comparison with two lines of empirical evidence, patterns of lag zero cross correlations with distance and geographical clustering of defoliation time series, simulations from the spatially explicit lattice model suggested two mechanisms for the observed spatial synchrony. A spatially autocorrelated Moran effect produced the decreasing pattern of cross correlations with distance. A relatively high dispersal rate apparently produced the observed east–west target pattern of clusters. Because of the admittedly qualitative nature of our evidence from cluster analyses, we are unable to mount a strong case for the effects of dispersal without further evidence. Nevertheless, the dynamics of spruce budworm outbreaks in eastern North America appear to be driven by the combined effects of a regional stochastic disturbance and the dispersal behavior of the species, which serve together to entrain its local populations across the region.

ACKNOWLEDGMENTS

We thank Greg Dwyer, Marcel Holyoak, Alison Hunter, Judith Myers, and Jan Volney for their helpful comments on

the manuscript. We also thank Richard Birdsey, program manager of the Northern Stations Global Change Research Program of the USDA Forest Service, for providing support for this research.

Literature Cited

Barbour, D. A. 1990. Synchronous fluctuations in spatially separated populations of cyclic forest insects. Pages 339–346 *in* A. D. Watt, S. R. Leather, M. D. Hunter and N. A. Kidd, editors. Population dynamics of forest insects. Intercept Ltd., Andover, UK.

Blais, J. R. 1985. The ecology of the eastern spruce budworm: a review and discussion. Pages 49–59 *in* C. J. Sanders, R. W. Stark, E. J. Mullins, and J. Murphy, editors. Recent advances in spruce budworms research. Canadian Forestry Service, Ottawa, Ontario, Canada.

Box, G. E. P., and G. M. Jenkins. 1976. Time series analysis, forecasting and control. Second edition. Holden-Day, San Francisco, California, USA.

Clark, W. C., D. D. Jones, and C. S. Holling. 1979. Lessons for ecological policy design. Ecological Modelling **7**:1–53.

Dennis, B., and M. L. Taper. 1994. Density dependence in time series observations of natural populations: estimation and testing. Ecological Monographs **64**:205–224.

Deutsch, C. V., and A. G. Journel. 1992. GSLIB. Geostatistical software library and user's guide. Oxford University Press, New York, New York, USA.

Dobesburger, E. J., K. P. Lim, and A. G. Raske. 1983. Spruce budworm moth flight from New Brunswick to Newfoundland. Canadian Entomologist **115**:1641–1645.

Everitt, B. 1980. Cluster analysis. Second edition. Halsted Press, New York, New York, USA.

Goovaerts, P. 1997. Geostatistics for natural resources evaluation. Oxford University Press, New York, New York, USA.

Greenbank, D. O. 1956. The role of climate and dispersal in the initiation of outbreaks of the spruce budworm in New Brunswick. I. The role of climate. Canadian Journal of Zoology **34**:453–476.

Greenbank, D. O., G. W. Schaefer, and F. R. S. Rainey. 1980. Spruce budworm moth flight and dispersal: new understanding from canopy observations, radar, and aircraft. Memoirs of the Entomological Society of Canada, Number **110**:1–49.

Grenfell, B. T., K. Wilson, B. F. Finkenstädt, T. N. Coulson, S. Murray, S. D. Albon, J. M. Pemberton, T. H. Clutton-Brock, and M. J. Crawley. 1998. Noise and determinism in synchronized sheep dynamics. Nature **39**:674–677.

Hanski, I., and D. Simberloff. 1997. The metapopulation approach, its history, conceptual domain, and application to conservation. Pages 5–26 *in* I. A. Hanski and M. E. Gilpin, editors. Metapopulation biology. Ecology, genetics, and evolution. Academic Press, San Diego, California, USA.

Hanski, I., and I. P. Woiwod. 1993. Spatial synchrony in the dynamics of moth and aphid populations. Journal of Animal Ecology **62**:656–668.

Hardy, Y., A. Lafond, and L. Hamel. 1983. The epidemiology of the current spruce budworm outbreak in Quebec. Forest Science **29**:715–725.

Hardy, Y., M. Mainville, and D. M. Schmitt. 1986. An atlas of spruce budworm defoliation in eastern North America, 1938–80. USDA Forest Service Miscellaneous Publication Number 1449. USDA Forest Service, Washington, D.C., USA.

Hawkins, B. A., and M. Holyoak. 1998. Transcontinental crashes of insect populations? American Naturalist **152**: 480–484.

Haydon, D., and H. Steen. 1997. The effects of large- and small-scale random events on the synchrony of metapopulation dynamics: a theoretical analysis. Proceedings of the Royal Society of London, B **264**:1375–1381.

Howse, G. M. 1995. Forest insect pests in the Ontario region. Pages 41–57 *in* J. A. Armstrong and W. G. H. Ives, editors. Forest insect pests in Canada. Natural Resources Canada, Canadian Forest Service, Ottawa, Ontario, Canada.

Howse, G. M., J. H. Meating, and J. J. Churcher. 1995. Insect control in Ontario, 1974–1987. Pages 679–699 *in* J. A. Armstrong and W. G. H. Ives, editors. Forest insect pests in Canada. Natural Resources Canada, Canadian Forest Service, Ottawa, Ontario, Canada.

Isaaks, E. H., and R. M. Srivastava. 1989. An introduction to applied geostatistics. Oxford University Press, New York, New York, USA.

Kettela, E. G. 1983. A cartographic history of spruce budworm defoliation from 1967 to 1981 in eastern North America. Canadian Forestry Service, Information report DPC-X-14. Canadian Forestry Service, Ottawa, Ontario, Canada.

Lachance, D. 1995. Forest insect pests in the Quebec region. Pages 27–39 *in* J. A. Armstrong and W. G. H. Ives, editors. Forest insect pests in Canada. Natural Resources Canada, Canadian Forest Service, Ottawa, Ontario, Canada.

Liebhold, A. M., and J. S. Elkinton. 1989. Characterizing spatial patterns of gypsy moth regional defoliation. Forest Science **35**:557–568.

Lindström, J., E. Ranta, and H. Lindén. 1996. Large-scale synchrony in the dynamics of capercaillie, black grouse and hazel grouse populations in Finland. Oikos **76**:221–227.

Mattson, W. J., G. A. Simmons, and J. A. Witter. 1988. The spruce budworm in eastern North America. Pages 310–331 *in* A. A. Berryman, editor. Dynamics of forest insect populations. Patterns, causes and implications. Plenum Press, New York, New York, USA.

Mearns, L. O., R. W. Katz, and S. H. Schneider. 1984. Extreme high-temperature events: changes in their probabilities with changes in mean temperature. Journal of Climate and Applied Meteorology **23**:1601–1613.

Moran, P. A. P. 1953*a*. The statistical analysis of the Canadian lynx cycle. I. Structure and prediction. Australian Journal of Zoology **1**:163–173.

Moran, P. A. P. 1953*b*. The statistical analysis of the Canadian lynx cycle. II. Synchronization and meteorology. Australian Journal of Zoology **1**:291–298.

Myers, J. H. 1988. Can a general hypothesis explain population cycles in forest Lepidoptera? Advances in Ecological Research **18**:179–242.

Myers, J. H. 1993. Population outbreaks in forest Lepidoptera. American Scientist **81**:240–251.

Myers, J. H. 1998. Synchrony in outbreaks of forest Lepidoptera: a possible example of the Moran effect. Ecology **79**:1111–1117.

Pollard, E. 1991. Synchrony of population fluctuations: the dominant influence of widespread factors on local butterfly populations. Oikos **60**:7–10.

Pollard, E., C. A. M. van Swaay, and T. J. Yates. 1993. Changes in butterfly numbers in Britain and the Netherlands, 1990–91. Ecological Entomology **18**:93–94.

Ralston, M. L., and R. I. Jennrich. 1978. DUD, a derivative-free algorithm for nonlinear least squares. Technometrics **20**:7–14.

Ranta, E., V. Kaitala, J. Lindström, and E. Helle. 1997*a*. The Moran effect and synchrony in population dynamics. Oikos **78**:136–142.

Ranta, E., V. Kaitala, J. Lindström, and H. Lindén. 1995*a*. Synchrony in population dynamics. Proceedings of the Royal Society of London B **262**:113–118.

Ranta, E., J. Lindström, and H. Lindén. 1995*b*. Synchrony in tetraonid dynamics. Journal of Animal Ecology **64**:767–776.

Ranta, E., V. Kaitala, and P. Lundberg. 1997*b*. The spatial

dimension in population fluctuations. Science **278**:1621–1623.
Régnière, J., and T. J. Lysyk. 1995. Population dynamics of the spruce budworm, *Choristoneura fumiferana*. Pages 95–105 *in* J. A. Armstrong and W. G. H. Ives, editors. Forest insect pests in Canada. Natural Resources Canada, Canadian Forest Service, Ottawa, Ontario, Canada.
Royama, T. 1984. Population dynamics of the spruce budworm *Choristoneura fumiferana*. Ecological Monographs **54**:429–462.
Royama, T. 1992. Analytical population dynamics. Chapman and Hall, London, UK.
SAS Institute. 1990. SAS/STAT User's Guide, Version 6. Fourth Edition. SAS Institute, Cary, North Carolina, USA.
Shepherd, R. F., D. D. Bennett, J. W. Dale, S. Tunnock, R. E. Dolph, and R. W. Thier. 1988. Evidence of synchronized cycles in outbreak patterns of douglas-fir tussock moth, *Orgyia pseudotsugata*. Memoirs of the Entomological Society of Canada **146**:107–121.
Spangler, W. M. L., and R. L. Jenne. 1990. World monthly surface station climatology (and associated datasets). National Center for Atmospheric Research, Boulder, Colorado, USA.
Sutcliffe, O. L., C. D. Thomas, and D. Moss. 1996. Spatial synchrony and asynchrony in butterfly population dynamics. Journal of Animal Ecology **65**:85–95.
Swetnam, T. W., and A. M. Lynch. 1993. Multicentury, regional-scale patterns of western spruce budworm outbreaks. Ecological Monographs **63**:399–424.
Thomas, C. D. 1991. Spatial and temporal variability in a butterfly population. Oecologia **87**:577–580.
Thomas, C. D., and I. Hanski. 1997. Butterfly metapopulations. Pages 359–386 *in* I. A. Hanski and M. E. Gilpin, editors. Metapopulation biology. Ecology, genetics, and evolution. Academic Press, San Diego, California, USA.
Walsh, J. E., M. B. Richman, and D. W. Allen. 1982. Spatial coherence of monthly precipitation in the United States. Monthly Weather Review **110**:272–286.
Ward, J. H. 1963. Hierarchical grouping to optimize an objective function. Journal of the American Statistical Association **58**:236–244.
Webb, F. E., J. R. Blais, and R. W. Nash. 1961. A cartographic history of spruce budworm outbreaks and aerial forest spraying in the Atlantic region of North America, 1949–1959. Canadian Entomologist **93**:360–379.
Wellington, W. G., J. J. Fettes, K. B. Turner, and R. M. Belyea. 1950. Physical and biological indicators of the development of outbreaks of the spruce budworm, *Choristoneura fumiferana* (Clem.). Canadian Journal of Research, Section D Zoological Science **28**:308–331.
Wiens, J. A. 1997. Metapopulation dynamics and landscape ecology. Pages 43–62 *in* I. A. Hanski and M. E. Gilpin, editors. Metapopulation biology. Ecology, genetics, and evolution. Academic Press, San Diego, California, USA.
Williams, D. W., and A. M. Liebhold. 1995. Influence of weather on the synchrony of gypsy moth outbreaks in New England. Environmental Entomology **24**:987–995.
Williams, D. W., and A. M. Liebhold. 1997. Latitudinal shifts in spruce budworm (Lepidoptera: Tortricidae) outbreaks and spruce-fir forest distributions with climate change. Acta Phytopathologica et Entomologica Hungarica **32**:205–215.
Ydenberg, R. C. 1987. Nomadic predators and geographical synchrony in microtine population cycles. Oikos **50**:270–272.